*Proc. Natl. Acad. Sci. USA*
Vol. 92, pp. 1841–1845, March 1995
Immunology

# Hydrodynamic studies of a complex between the Fc fragment of human IgE and a soluble fragment of the FcεRI α chain

(stoichiometry/hydrodynamic modeling/allergy)

MAURA B. KEOWN*, RODOLFO GHIRLANDO†, ROBERT J. YOUNG*, ANDREW J. BEAVIL*, RAYMOND J. OWENS‡, STEPHEN J. PERKINS¶, BRIAN J. SUTTON*, AND HANNAH J. GOULD*§

*The Randall Institute, King's College London, 26-29 Drury Lane, London WC2B 5RL, United Kingdom; †National Institute of Diabetes, Digestive and Kidney Diseases, National Institutes of Health, Bethesda, MD 20892; ‡Celltech Ltd., 216 Bath Road, Slough SL1 4EN, United Kingdom; and ¶Department of Biochemistry and Molecular Biology, Royal Free Hospital School of Medicine, Rowland Hill Street, London NW3 2PF, United Kingdom

*Communicated by David R. Davies, National Institutes of Health, Bethesda, MD, November 10, 1994 (received for review May 24, 1994)*

**ABSTRACT** **The interaction between immunoglobulin E (IgE) and its high-affinity receptor FcεRI is central to allergic disease. The binding site for FcεRI lies in the third constant region domain of the ε heavy chain of IgE (Cε3). Identical epitopes on the two Cε3 domains in the IgE–Fc are predicted to be on opposite sides of the structure, and therefore each could bind independently to a receptor molecule. Titrations, however, reveal that the IgE–Fc forms an equimolar complex with a soluble fragment of the FcεRI α chain (sFcεRIα), and the molecular weight of the complex, as determined by sedimentation equilibrium, confirms this stoichiometry. The measured sedimentation coefficients of the two ligands are in good agreement with computed values for a compact IgE–Fc and an elongated sFcεRIα structure. The calculated sedimentation coefficients for possible models of a 1:1 complex lead to exclusion of all highly extended geometries for the complex. Possible explanations for the paradoxical stoichiometry of the IgE–Fc/sFcεRIα complex, in terms of the curved shape of IgE, a conformational change in IgE when the receptor binds, and steric interference between two molecules of FcεRI binding to identical sites, are discussed.**

Immunoglobulin E (IgE) is distinguished from other antibody classes by its ε heavy chain. Its high-affinity receptor, FcεRI, is primarily expressed on the surface of mast cells and basophils and is thought to be of major importance in IgE-dependent functions, which are relevant to the etiology of allergic disease (1). The affinity of IgE for FcεRI ($K_a = 10^{10}$ $M^{-1}$) is more than an order of magnitude greater than that for antibodies of any other class with any known Fc receptor (2). The stability of the interaction may be inseparable from the role of IgE in immediate hypersensitivity reactions.

FcεRI binds to the Fc region of IgE (3, 4), which is a disulfide-linked dimer of a polypeptide chain, comprising the second, third, and fourth constant region domains, Cε2–Cε4, of the ε heavy chain. This region is thought to be made up of two associated immunoglobulin domains, $(Cε2)_2$ and $(Cε4)_2$, with two widely separated (Cε3) domains between them (1). FcεRI is made up of four chains (α, β, $γ_2$), but the extracellular portion of the α chain, comprising two immunoglobulin-like domains, is sufficient to generate full binding affinity (5, 6). The binding sites have been further mapped to Cε3 in the IgE–Fc (refs. 7–9; reviewed in refs. 1 and 10) and to the second, membrane-proximal immunoglobulin-like domain, α2, in the α chain (refs. 11 and 12; reviewed in ref. 1). Although the binding sites in IgE and FcεRI are thus roughly defined, little is known about the arrangement of the two ligands in the complex. The stability of the complex makes it amenable to study by hydrodynamic methods in dilute solution. Here we have used recombinant protein fragments, representing the IgE–Fc and the extracellular portion of the FcεRI α chain, to determine the binding stoichiometry and to test various structural models of the complex.

## MATERIALS AND METHODS

**Recombinant Human IgE–Fc and Soluble Fragment of the FcεRI α Chain (sFcεRIα).** Preparation of the IgE–Fc is described in detail elsewhere (13) and that of sFcεRIα resembles $α_{trunc}$ of Blank *et al.* (6) (unpublished data). Molar absorptivities of 95,700 and 54,700 $M^{-1}·cm^{-1}$, respectively, at 280 nm have been calculated from the amino acid compositions (14).

**Titration of IgE–Fc with sFcεRIα.** Titrations were carried out by mixing $10^{-6}$ M solutions of the two proteins in various proportions, keeping the total molar protein concentration constant. Because of the extremely slow dissociation rate of the complex, the concentration could be determined by separating the unbound components from the complex by HPLC chromatography on a Zorbax Bioseries column (i.d., 250 × 100 mm) in 50 mM sodium phosphate/150 mM sodium chloride/500 mM arginine chloride, pH 6.0. The isolated complex was estimated spectrophotometrically at 280 nm.

**Preparation of the IgE–Fc/sFcεRIα Complex.** The IgE–Fc and sFcεRIα were mixed in equimolar proportions and the complex was purified by HPLC. Samples were concentrated with ultrafiltration with Diaflo YM10 membranes (Amicon) and dialyzed into PBS.

**Electrophoresis.** The free ligands and the complex were analyzed by electrophoresis on SDS/15% polyacrylamide gels under nonreducing conditions (15). Proteins were stained by using the ISS pro-blue staining system (NBS Biologicals) and apparent molecular weights based on the migration of colored protein markers (range, 14,300–200,000; Amersham).

**Sedimentation Equilibrium Studies.** Sedimentation equilibrium experiments at 4.0°C in a Beckman Optima XL-A analytical ultracentrifuge were conducted using an An60Ti rotor at three or more different speeds for each sample, ranging from 11,000 to 17,000 rpm for the IgE–Fc and complex and from 18,000 to 22,000 rpm for the sFcεRIα. Data were acquired as an average of 20 absorbance measurements at 280 nm at a radial interval of 0.001 cm with a solution column of 2 mm. Equilibrium was usually established within 10 h. Initial protein concentrations corresponded to a measured $A_{280}$ of ≈0.3 for the IgE–Fc and the complex and 0.6 for sFcεRIα. The data were analyzed assuming a single ideal solute, to obtain the buoyant molecular weight $M(1 - \bar{\nu}\rho)$ by the following equation (Optima XL-A data analysis software, version 2.0, Beckman running under Origin 2.8):

The publication costs of this article were defrayed in part by page charge payment. This article must therefore be hereby marked "*advertisement*" in accordance with 18 U.S.C. §1734 solely to indicate this fact.

Abbreviations: Cε2, Cε3, and Cε4, second, third, and fourth constant region domains of ε heavy chain of IgE; sFcεRIα, soluble fragment of FcεRI α chain.

§To whom reprint requests should be addressed.

$$A_r = \exp[\ln(A_o) + (\omega^2/2RT)M(1 - \bar{\nu}\rho)(r^2 - r_0^2)],$$

where $A_o$ is the absorbance at a reference point $r_o$, $A_r$ is the absorbance as a function of the radius $r$ in cm, $\omega$ is speed of rotation in radians/sec, M is the molecular weight of the protein, $R$ is the gas constant, $T$ is the absolute temperature, $\bar{\nu}$ is the partial molar volume of the protein in $cm^3 \cdot g^{-1}$, and $\rho$ is the density of the solution in $g \cdot ml^{-1}$. The values of $M(1 - \bar{\nu}\rho)$, obtained from at least two separate protein samples run at various speeds, were averaged to yield the experimental values of $M(1 - \bar{\nu}\rho)$. In all cases, the residuals, obtained by subtracting the calculated best fit from the experimental data, had a random distribution around 0 ($\pm < 0.020$) as a function of the radius. The density of the solution was measured at 20.00°C (Anton Paar DMA58 densitometer) and corrected to 4.0°C with standard tables.

**Sedimentation Velocity Measurements.** Sedimentation velocity experiments were performed at 20.0°C on the Beckman Optima XL-A ultracentrifuge using an An60Ti rotor at 40,000 rpm (IgE–Fc and complex), 45,000 rpm (IgE–Fc), and 50,000 rpm (sFcεRIα) with double sector cells. In all cases, data for two protein concentrations ($A_{280}$, 0.30–0.85) were simultaneously collected at 280 nm and at shorter wavelength (absorbance of 1.0). Scans were recorded every 10 min for 3 h and analyzed with the program XLAVEL (Beckman) to yield an uncorrected sedimentation coefficient, $s$. Each measurement was performed at least twice. The density of water at 20.00°C and the viscosities of water and PBS were obtained from the literature. $S$ was corrected to $s^0_{20,w}$.

**Hydrodynamic Modeling of IgE–Fc, sFcεRIα, and the Complex.** Sedimentation coefficients ($s^0_{20,w}$) were computed on the basis of models of the structure of the IgE–Fc (16, 17) and on a model of sFcεRIα based on the crystal structure of CD2 (18). Other models of sFcεRIα have been reported (e.g., see ref. 19) but would not be expected to yield significantly different sedimentation coefficients, as the methods used here are sensitive only to gross conformation. The possibility that IgE–Fc could exhibit bending within the Cε2–Cε3 linker region was investigated by generating a series of models with successive rotations and translations of $(C\varepsilon2)_2$ relative to $(C\varepsilon3)_2$. The domains were rotated about an axis through the two Asp-330 $C_\alpha$ atoms and translated toward the Cε3 domains.

Carbohydrate chains were modeled on those found in the human Fc crystal structure (20). These were attached to the putative carbohydrate sites on the proteins by using Insight II molecular graphics software (Biosym Technologies, San Diego).

To generate the hydrodynamic models, the molecular models were approximated by an ensemble of spheres using a program in which the model was placed in a three-dimensional grid of cubes (21). The cubes were included as the building blocks of the hydrodynamic model if they contained an α-carbon atom or a Cl carbohydrate atom. The dimensions of the cubes were optimized so that the total volume of the cubes equaled that of the dry volume of the protein molecule calculated from the composition (95.5 and 40.5 $nm^3$ for IgE–Fc and sFcεRIα, respectively). The volumes were then increased to allow for a hydration shell, assumed to comprise 0.3 g of water per g of glycoprotein and an electrostricted volume of 0.0245 $nm^3$ per bound water molecule (14, 21). The resulting models were assigned coordinates to produce the final hydrodynamic models, consisting of nonoverlapping spheres placed at the center of each cube, which now had sides of 0.694 nm. Hydrodynamic calculations were performed by the modified Oseen tensor procedure using the program GENDIA (22, 23) with up to 407 spheres.

## RESULTS

**Characterization of IgE–Fc and sFcεRIα.** The purity of the preparations of the recombinant IgE–Fc and sFcεRIα fragments was assessed by PAGE in SDS before and after treatment with N-glycanase under denaturing conditions to remove all N-linked carbohydrate (Fig. 1). The IgE–Fc preparation migrated as a single component with an apparent molecular weight of 75,000. The sFcεRIα migrated as a single broad zone, spanning an apparent molecular weight range of 38,000–56,000. After deglycosylation, the apparent molecular weight ($M_r$) of the IgE–Fc was reduced to 72,500 (cf. $M_r$ 72,000 calculated from the amino acid composition), while the deglycosylated sFcεRIα was reduced to 20,000 (calculated $M_r$, 21,000).

**Stoichiometry of the Complex.** Titrations were carried out to determine the stoichiometry of the interaction between the IgE–Fc and sFcεRIα. Fig. 2 shows a continuous variation titration, in which the total molar protein concentration was kept constant and the proportions of the two components were varied. The IgE–Fc/sFcεRIα complex was separated from the free ligands by gel filtration (Fig. 2*A*). The dissociation rate of this complex is negligible compared to the elution time. Equivalence is reached at a mole ratio of 1:1 (Fig. 2*B*). These experiments also showed total binding of either component in the presence of an excess of the other, indicating that both preparations were fully folded and active.

**Molecular Weight Determinations.** To confirm that the complex contains equimolar proportions of the two constituents and determine whether it is made up of one polypeptide chain of each or a higher multiple, molecular weight determination by sedimentation equilibrium was undertaken.

The sedimentation equilibrium distributions (Fig. 3 *A* and *B*) for the two separate components show that they are monodisperse within the experimental precision of the method. From these results, we obtain the reduced or buoyant molecular weight $M(1 - \bar{\nu}\rho)$. The value of $\bar{\nu}$ was calculated from the amino acid and carbohydrate composition (14), assuming that the carbohydrate chains are of the complex biantennary type, with a core composition of $Gal_2Man_3GlcNAc_4$ (20, 24).

The main uncertainties are the occupancy of the glycosylation sites and the amount, if any, of sialic acid in sFcεRIα. The amino acid sequence reveals a maximum of seven glycosylation sites in sFcεRIα. Using the relationship between the reduced molecular weight of sFcεRIα and that of the sum of its protein (p) and carbohydrate (c) constituents,

$$M(1 - \bar{\nu}\rho) = M_p(1 - \bar{\nu}_p\rho) + M_c(1 - \bar{\nu}_c\rho), \quad [1]$$

we can examine the effect of varying $\bar{\nu}_c$ within the possible limits of carbohydrate composition on the value of $M_c$—that is to say, the occupancy of the available glycosylation sites. With zero, one, and two sialic acid residues per carbohydrate chain, $\bar{\nu}_c$ is 0.644, 0.649, and 0.653 $cm^3 \cdot g^{-1}$, respectively. The corresponding values of $M_c$ given by Eq. **1** are then 13,700, 13,900, and 14,100, and $M_p$ = 21,000. Thus, we can define the

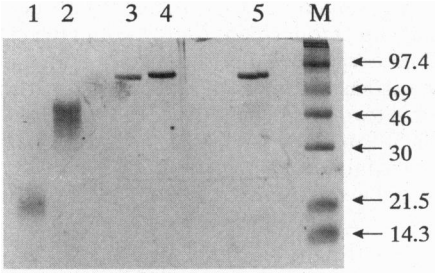


FIG. 1. Gel electrophoresis of IgE–Fc, sFcεRIα, and their complex. Lanes: 1, deglycosylated sFcεRIα; 2, sFcεRIα; 3, deglycosylated IgE–Fc; 4, IgE–Fc; 5, complex between the IgE–Fc and sFcεRI (dissociated into the two ligands); M, molecular weight markers ($\times 10^{-3}$).

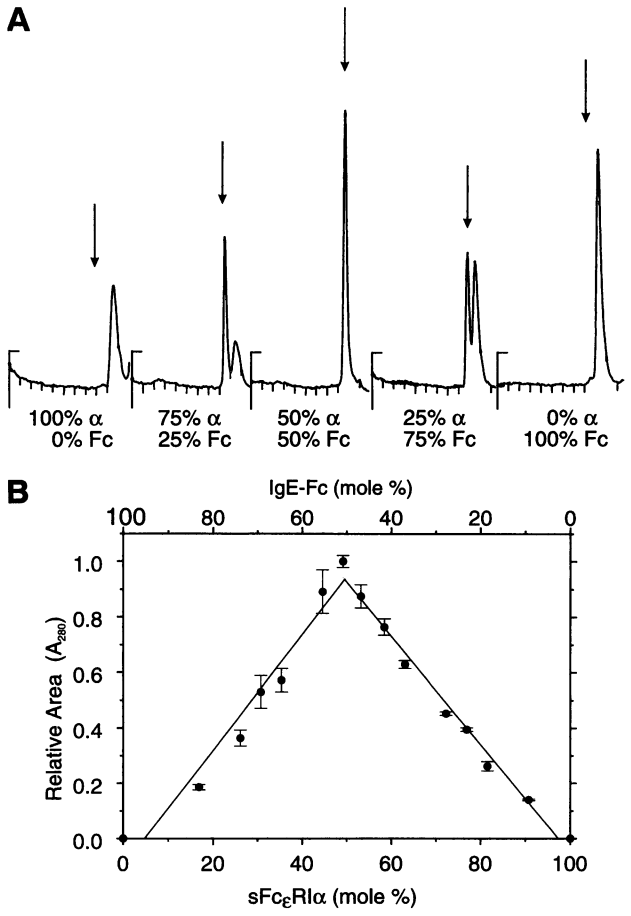


FIG. 2. Stoichiometry of the complex between IgE–Fc and sFcεRIα. (*A*) HPLC profiles at selected molar ratios; arrow denotes the expected position of the complex. (*B*) Relative abundance of complex as a function of the molar ratio of IgE–Fc/sFcεRIα. Straight lines represent the best linear fit for data between 0–50% and 50–100% mol fraction of sFcεRIα.

molecular weight of sFcεRIα within the above limits as 34,400 ± 1400. If $M_c$ is 13,900 ± 1400 and the molecular weights of the individual carbohydrate chains are 1600, 1900, 2200 (core carbohydrate with zero, one, or two sialic acid residues), it seems that to a good approximation all seven of the putative glycosylation sites are occupied with an average sialic acid content of about one residue per chain. The carbohydrate content for the α-chain fragment is therefore 40%, in good agreement with the value of 32% determined for the whole α chain isolated from rat basophilic leukemia cells (25).

The molecular weight determination for the IgE–Fc is straightforward, since both glycosylation sites are occupied and there appears to be little sialic acid (13). Substituting the calculated values of $M_p$ = 72,000, $\bar{\nu}_p$ = 0.730 g·cm$^{-3}$, $M_c$ = 3200, and $\bar{\nu}_c$ = 0.644 g·cm$^{-3}$ into Eq. **1**, the experimental value of $M(1 - \bar{\nu}\rho)$ = 19,700 ± 800 delivers a molecular weight of 73,600 ± 2800.

We now consider the sedimentation equilibrium of the complex (Fig. 3*C*). This is again monodisperse within experimental precision. We note first that the derived composition of the complex does not depend on the accuracy with which the partial specific volumes are known—that is to say, on the carbohydrate content of the constituents—because the buoyant molecular weight, determined from the sedimentation equilibrium distribution, is the sum of the buoyant molecular weights of the constituent glycoproteins. The buoyant molecular weights of the IgE–Fc and sFcεRIα are 19,700 and 10,200, respectively, and that of the complex is 29,400. Thus, the complex contains one subunit of each kind. From the inferred carbohydrate contents of the separate components and the corresponding partial specific volumes, we now obtain a partial specific volume of 0.718 cm$^3$·g$^{-1}$ for the complex, corresponding to a molecular weight of 106,400 ± 2700.

**Hydrodynamic Modeling of IgE–Fc, sFcεRIα, and Their Complex.** Sedimentation coefficients ($s^0_{20,w}$) were determined for the three species (Table 1) and compared to those calculated from models. The more recent model of Helm *et al.* (17) for the IgE–Fc embodies changes in the Cε2 domain that are below the level of resolution of the hydrodynamic technique but also has an extended region between Cε2 and Cε3. This results in a calculated sedimentation coefficient of 4.38 S, which agrees less well with our experimental data than does the model of Padlan and Davies (16) with its more compact arrangement of Cε2 relative to Cε3.

It has been suggested that IgE may be bent (26, 27), and this distortion could occur, at least in part, within the Cε2–Cε3 linker. The consequences of this were investigated by using the extended model. Rotation of Cε2 relative to Cε3 by between 60° and 120° was found to lead to a calculated sedimentation coefficient compatible with the observed experimental value, and the acceptable range of rotation angles increased as Cε2 was translated toward Cε3. However, imposition of the additional constraint of the observed radius of gyration from x-ray scattering, $R_G$ = 3.52 ± 0.14 nm (A.J.B. and S.J.P., unpublished results), excludes all models except those with a rotation of 90° ± 10° and a translation of 0.6 ± 0.2 nm ($R_G$ = 3.58 nm). The original compact model of Padlan and Davies was, however, equally compatible with the data ($R_G$ = 3.68 nm), and for this reason both models of the IgE–Fc were considered in modeling of the complex. The models chosen for the IgE–Fc and sFcεRIα led to calculated values of 4.66 S for the compact model (16) and 4.55 S for the bent model (based on ref. 17), of the IgE–Fc and 2.74 S for sFcεRIα (1), each with a precision of ±0.1 S (refs. 26–28; see Table 1).

A number of possible models for the complex can now be envisaged (Fig. 4). These include the cases in which the constituents associate at their ends, with their long axes parallel (Fig. 4 *a* and *b*) or orthogonal (Fig. 4 *c–f*). Models in which the contacts were made at the Cε2, Cε3, or Cε4 domains in IgE–Fc, to generate extended structures with no domain overlap, gave calculated sedimentation coefficients of 5.06–5.35 S for the planar compact model and 4.67–5.50 S for the bent model. A second set of models, in which either one or no domain of sFcεRIα extended beyond the IgE–Fc domains, gave values of 5.62–5.84 S (Fig. 4 *g–j*) in both cases. The difference between calculated and experimental values determined from Oseen tensors is not expected to exceed ±0.26 S (21). By this criterion we can exclude all such models as exemplified by Fig. 4 *a–f*, except *e* and *f* in the case of the bent model. Those shown in Fig. 4 *g–j* are compatible with the experimental values.

## DISCUSSION

The aim of this study was to determine the composition and the gross shape of the complex between the IgE–Fc and the α chain of FcεRI in solution. IgE is the natural ligand for FcεRI, but the IgE–Fc binds with about the same affinity to this receptor (13) and it was preferred to whole IgE for hydrodynamic studies because of its smaller size and thus greater confidence in modeling a 6-domain rather than a 14-domain structure. sFcεRIα represents the whole extracellular region of the α chain but, unlike the intact α chain, is soluble in the absence of detergents. Our results demonstrate that the IgE–Fc and sFcεRIα form a 1:1 complex.

Antibodies consist of two identical heavy and light chains, and in the Fc region of IgG the two heavy chains form a structure with a twofold axis of symmetry; thus, each structural

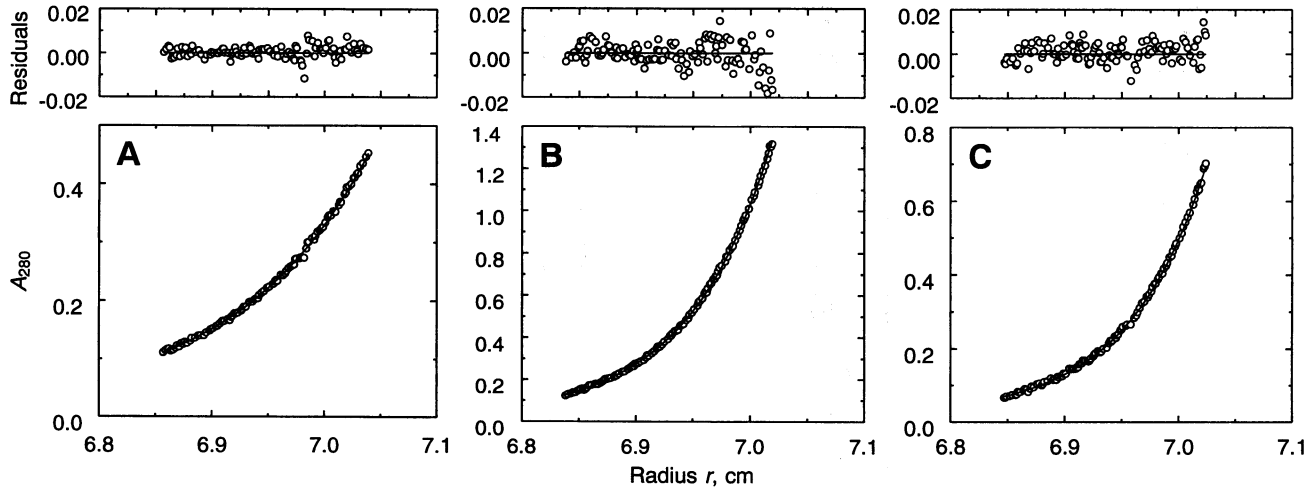


FIG. 3. Sedimentation equilibrium data for the IgE–Fc, sFcεRIα, and the complex, shown as a distribution of $A_{280}$ at equilibrium. Data were collected at 4°C and 11,000 rpm for IgE–Fc (*A*), 20,000 rpm for sFcεRIα (*B*), and 12,000 rpm for the complex (*C*). Data are analyzed for the best single component (M − $\bar{\nu}\rho$) fit, shown as a line through the experimental points. Corresponding distributions of the residuals are shown above each plot.

element of one heavy chain in the Fc is related to an identical element on the other chain by a rotation of 180° about its longitudinal axis (20). The binding of the neonatal IgG–Fc receptor, FcγRn (29), and of protein A (20) to IgG exemplifies the formation of complexes with a stoichiometry of 2:1. The IgE–Fc contains one more domain pair (Cε2) than the IgG–Fc. If its structure has similar symmetry, and given that each receptor can bind only one antibody molecule (ref. 30 and results herein), we need to explain why a 2:1 sFcεRIα/IgE–Fc complex is not formed.

Early studies by Kanellopoulos *et al.* (25) revealed that IgE is engaged by only one molecule of FcεRI on the membrane surface. From a functional standpoint this result is unsurprising: the proper functioning of the cellular immune system precludes cross-linking of two cell surface receptors by an antibody, for then the cell could be activated in the absence of antigen. There should therefore be only one binding site in IgE to meet the demands of cell signaling. This consideration does not apply to the binding of FcγRn or protein A to IgG.

The simplest explanation is that there are in fact two equivalent sites on opposite sides of the antibody, but only one can be occupied by cell-bound receptor because the other faces away from the cell membrane or is in some way occluded by its proximity to the membrane. In this case, the stoichiometry at the cell surface would be 1:1, but that of receptor binding to IgE in solution would be 2:1. This prediction is not borne out by recent studies of complex formation between sFcεRIα and whole IgE. According to Ra *et al.* (31), the ratio is <1:1, while according to Robertson it is 1:1 (11). Our results confirm the latter conclusion and exclude the possibility that there might be multiple copies of both ligands in the complex. The smaller size of the IgE–Fc, compared to IgE, places greater constraints on possible models of a 1:1 complex.

Three possible explanations for the observed 1:1 stoichiometry may be envisaged: (*i*) IgE in solution is not planar but bent, so that the N-terminal ends of the Fab regions are much closer to the C-terminal end of the Fc than they would be in a flat structure (refs. 26 and 27; A.J.B. and S.J.P., unpublished results). In the absence of more detailed structural information, this distortion is generally represented as being evenly distributed between all the linker regions separating the immunoglobulin domains (1, 26, 27). A binding site on the convex surface of the IgE, say on Cε3, might then be accessible to the receptor, while the Fab arms, together with $(Cε2)_2$ and $(Cε4)_2$ may sterically hinder binding to the concave surface. The IgE–Fc could retain this bent structure (as considered above). However, we have made a disulfide-bridged dimer of a subfragment of the IgE–Fc, consisting of only the Cε3 and Cε4 domains, which should thus resemble the planar IgG–Fc fragment and find that this species also forms a 1:1 complex with sFcεRIα (M.B.K. and R.G., unpublished results). Thus, bending cannot be the only aspect of the structure of the IgE–FcεRI complex to determine the stoichiometry.

(*ii*) Binding of the receptor may cause a conformational change in IgE that precludes the binding of a second receptor molecule. The Cε3 domains are expected to be remote from each other (as are Cγ2 domains in IgG–Fc), and it is unlikely that such a conformational change could be transmitted through the N-linked oligosaccharide chains that lie between them. However, the two ε chains do come close together in the region that links Cε3 to Cε2, owing to the interchain disulfide bond between the two Cys-328 residues near the border between Cε2 and Cε3 (the codon for Asp-330 is divided between the exons for Cε2 and Cε3), and such a region might be more susceptible to deformation upon binding to receptor.

(*iii*) Occupancy of one receptor binding site may prevent binding to the second site. This could occur if the receptor apposes or binds to IgE in any part of the structure where the two ε chains are in close proximity. All the available evidence maps the FcεRI binding site to the Cε3 domain(s), (refs. 7–9; reviewed in refs. 1 and 10), which are well separated from each other except in the Cε2/Cε3 linker region (17). If FcεRIα

Table 1. Sedimentation equilibrium and velocity data

| Sample | M(1 − $\bar{\nu}\rho$), g·mol$^{-1}$* | M, g·mol$^{-1}$† | $\bar{\nu}$, cm$^3$·g$^{-1}$‡ | Calculated M‡ | $s^0_{20,w}$* |
|---|---|---|---|---|---|
| IgE–Fc | 19,700 ± 800 (16) | 73,600 ± 2800 | 0.727 | 75,274 | 4.7 ± 0.1 (7) |
| sFcεRIα | 10,200 ± 400 (12) | 34,400 ± 1400 | 0.698 | 33,782 | 2.8 ± 0.1 (8) |
| Complex | 29,400 ± 800 (10) | 106,400 ± 2700 | 0.718 | 109,056 | 5.7 ± 0.05 (8) |

*Experimentally determined mean value based on *n* measurements (*n* is shown in parentheses) together with SD.
†Measured values of molecular weight based on the calculated partial specific volume, $\bar{\nu}$.
‡Calculated value based on the known amino acid composition and full occupancy of the glycosylation sites.

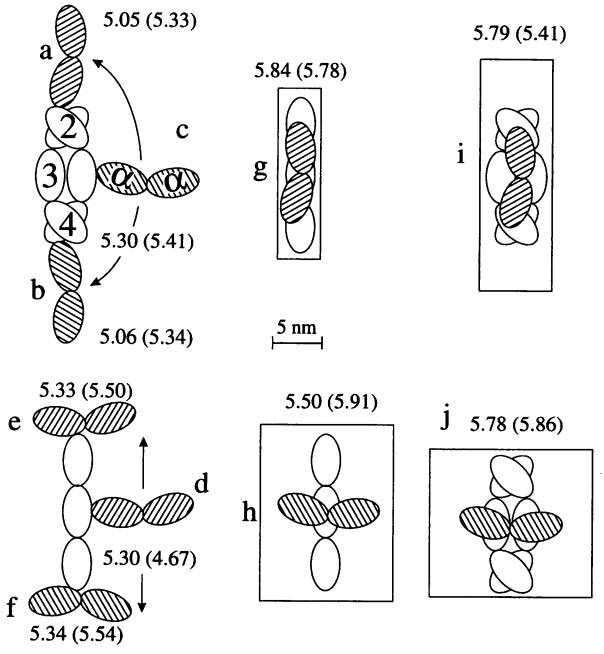


FIG. 4. Models of the IgE–Fc/sFcεRIα complex. Models of the IgE–Fc and sFcεRIα have been juxtaposed in a variety of ways and a selection of schematic models (IgE–Fc, open; FcεRIα, hatched) are shown. (*a–d*) End to end. (*e* and *f*) T-shaped models. (*g* and *h*) Receptor bound at the side of the IgE–Fc. (*i*) Long axes of the IgE–Fc and sFcεRIα parallel or antiparallel. (*j*) Long axes of the two ligands perpendicular. Models fall into three groups: extended models (*a–f*), compact models that have sFcεRIα bound to the sides (*g* and *h*), and those that have sFcεRIα bound on the planar surface (*i* and *j*). Arrows (*a–f*) indicate the range of positions of sFcεRIα relative to IgE–Fc that were considered. Boxes (*g–j*) define the limits on the position of sFcεRIα relative to IgE–Fc for which the calculated $s^0_{20,w}$ values are compatible with the experimental value—i.e., within ±0.3 S (combined experimental and computational errors) of $s^0_{20,w}$ = 5.7 S. Numbers are sedimentation coefficients calculated for the specific models shown; numbers in parentheses correspond to the model with a bent IgE–Fc.

comes close to Cε3 in this region, there may be room for only one molecule to bind.

The hydrodynamic evidence limits the range of possible models for the complex of IgE–Fc and sFcεRIα to those in which the domains of the IgE–Fc overlap with those of the sFcεRIα (Fig. 4 *g–j*), although two T-shaped models (Fig. 4 *e* and *f*) cannot be excluded on these grounds alone in the case of a bent model of the IgE–Fc. Bent forms can be excluded, however, if one accepts that the binding site is in Cε3. The two models in which the receptor is in contact only with the sides of the IgE–Fc (Fig. 4 *g* and *h*) are unlikely on the basis of the 1:1 stoichiometry of the complex. The most acceptable models on the evidence at present available to us, therefore, comprise the family in which the long axis of sFcεRIα is either parallel (Fig. 4*i*) or perpendicular (Fig. 4*j*) to the long axis of the IgE–Fc on the front face of IgE or in any intermediate orientation between these extremes.

We thank A. Ginsburg for the use of the densimeter, R. L. Beavil for drawing Fig. 4, and G. Felsenfeld and W. B. Gratzer for helpful discussions. This work was supported by a Collaborative Award in Science and Engineering Studentship to M.B.K., Medical Research Council (U.K.) and National Asthma Campaign (U.K.) project grants to B.J.S. and H.J.G., and Wellcome Trust project grants to S.J.P.

1. Sutton, B. J. & Gould, H. J. (1993) *Nature (London)* **366,** 421–428.
2. Ravetch, J. V. & Kinet, J.-P. (1991) *Annu. Rev. Immunol.* **9,** 457–492.
3. Stanworth, D. R., Humphrey, J. H., Bennich, H. & Johansson, S. G. (1968) *Lancet* **ii,** 17.
4. Ishizaka, K., Ishizaka, T. & Lee, E. H. (1970) *Immunochemistry* **7,** 687–702.
5. Hakimi, J., Seals, C., Kondas, J. A., Pettine, L., Danho, W. & Kochan, J. (1990) *J. Biol. Chem.* **265,** 22079–22081.
6. Blank, U., Ra, C. S. & Kinet, J.-P. (1991) *J. Biol. Chem.* **266,** 2639–2646.
7. Helm, B., Marsh, P., Vercelli, D., Padlan, E., Gould, H. & Geha, R. S. (1988) *Nature (London)* **331,** 180–183.
8. Nissim, A. & Eshhar, Z. (1992) *Mol. Immunol.* **29,** 1065–1072.
9. Basu, M., Hakimi, J., Dharm, E., Kondas, J. A., Tsien, W.-H., Pilson, R. S., Lin, P., Gilfillan, A., Haring, P., Braswell, E. H., Nettleton, M. Y. & Kochan, J. P. (1993) *J. Biol. Chem.* **269,** 13118–13127.
10. Beavil, A. J., Beavil, R. J., Chan, C. M. W., Cook, J. P. D., Gould, H. J., Henry, A. J., Owens, R. J., Shi, J., Sutton, B. J. & Young, R. J. (1993) *Biochem. Soc. Trans.* **21,** 968–972.
11. Robertson, M. W. (1993) *J. Biol. Chem.* **268,** 12736–12743.
12. Scarselli, E., Esposito, G. & Traboni, C. (1993) *FEBS Lett.* **329,** 223–226.
13. Young, R. J., Owens, R. J., Mackay, G. A., Chan, C. M. W., Shi, J., Hide, M., Francis, D. M., Henry, A. J., Sutton, B. J. & Gould, H. J. (1995) *Protein Eng.*, in press.
14. Perkins, S. J. (1986) *Eur. J. Biochem.* **157,** 169–180.
15. Laemmli, U. K. (1970) *Nature (London)* **277,** 680–685.
16. Padlan, E. A. & Davies, D. R. (1986) *Mol. Immunol.* **23,** 1063–1075.
17. Helm, B. A., Ling, Y., Teale, C., Padlan, E. A. & Bruggemann, M. (1991) *Eur. J. Immunol.* **21,** 1543–1548.
18. Jones, E. Y., Davis, S. J., Williams, A. F., Harlos, K. & Stuart, D. I. (1992) *Nature (London)* **360,** 232–239.
19. Padlan, E. A. & Helm, B. A. (1992) *Receptor* **2,** 129–144.
20. Deisenhofer, J. (1981) *Biochemistry* **20,** 2361–2370.
21. Perkins, S. J. (1989) in *Dynamic Properties of Biomolecular Assemblies*, eds. Harding, S. E. & Rowe, A. J. (Royal Soc. Chemistry, London), Chap. 15, pp. 226–245.
22. Garcia de la Torre, J. & Bloomfield, V. A. (1977) *Biopolymers* **16,** 1747–1763 and 1779–1793.
23. Garcia de la Torre, J. (1989) in *Dynamic Properties of Biomolecular Assemblies*, eds. Harding, S. E. & Rowe, A. J. (Royal Soc. Chemistry, Cambridge, U.K.), pp. 3–31.
24. LaCroix, E. L. & Froese, A. (1993) *Mol. Immunol.* **30,** 321–330.
25. Kanellopoulos, J. M., Liu, T. Y., Poy, G. & Metzger, H. (1980) *J. Biol. Chem.* **255,** 9060–9066.
26. Zheng, Y., Shopes, R., Holowka, D. & Baird, B. (1991) *Biochemistry* **30,** 9125–9132.
27. Zheng, Y., Shopes, B., Holowka, D. & Baird, B. (1992) *Biochemistry* **31,** 7446–7456.
28. Perkins, S. J., Smith, K. F., Kilpatrick, J. M., Volanakis, J. E. & Sim, R. B. (1993) *Biochem J.* **295,** 87–99.
29. Huber, A. H., Keeley, R. F., Gastinel, L. N. & Bjorkman, P. J. (1993) *J. Mol. Biol.* **230,** 1077–1083.
30. Mendoza, G. & Metzger, H. (1976) *Nature (London)* **264,** 548–550.
31. Ra, C., Kuromitsu, S., Hirose, T., Yasuda, S., Furuichi, K. & Okumura, K. (1993) *Int. Immunol.* **5,** 47–54.